

# Improving semi-device-independent randomness certification by entropy accumulation

Carles Roch i Carceller,<sup>1,2,\*</sup> Lucas Nunes Faria,<sup>1</sup> Zheng-Hao Liu,<sup>1</sup> Nicolò Sguerso,<sup>1</sup>  
Ulrik Lund Andersen,<sup>1</sup> Jonas Schou Neergaard-Nielsen,<sup>1</sup> and Jonatan Bohr Brask<sup>1,†</sup>

<sup>1</sup>*Center for Macroscopic Quantum States (bigQ), Department of Physics,  
Technical University of Denmark, 2800 Kongens Lyngby, Denmark*  
<sup>2</sup>*Physics Department, Lund University, Box 118, 22100 Lund, Sweden*

Certified randomness guaranteed to be unpredictable by adversaries is central to information security. The fundamental randomness inherent in quantum physics makes certification possible from devices that are only weakly characterised i.e. requiring little trust in their implementation. It was recently shown that the amount of certifiable randomness can be greatly improved using the so-called Entropy Accumulation Theorem generalised to prepare-and-measure settings. Furthermore, this approach allows a finite-size analysis which avoids assuming that all rounds are independent and identically distributed. Here, we demonstrate this improvement in semi-device-independent randomness certification from untrusted measurements.

## I. INTRODUCTION

Randomness is a fundamental resource [1] for a variety of applications in the modern world including information security [2, 3], simulations of physical systems [4–8], games, and gambling. Cryptographic protocols in particular require unpredictability relative to potential adversaries of the random numbers used to generate keys.

For pseudo-random number generators [9] and randomness generated from classical physical processes, certification of unpredictability requires assumptions about the information and computational power available to the adversaries. The inherent randomness of quantum measurements, on the other hand, enables randomness certification directly from fundamental physical laws and measurable properties of the devices used [10–13]. From a characterisation of states and measurements on a given system, the entropy (quantifying unpredictability) relative to any adversary constrained by quantum mechanics can be bounded. In fact, by exploiting quantum nonlocality [14], the need for a thorough characterisation can even be eliminated, allowing randomness certification in a black-box setting, provided the devices violate a Bell inequality [15–17]. This corresponds to a very strong level of security, known as device independence (DI), since minimal trust in the devices is required [18–22]. DI schemes, however, are also more technologically challenging to implement than device-dependent ones with well characterised devices. Hence, it is desirable to identify good trade-offs between ease of implementation and how little trust is required to certify randomness, i.e. to explore semi-DI quantum random number generators (QRNGs). A number of different prepare-and-measure schemes with partially characterised sources or measurements have been explored [23–45].

Randomness in a variable  $b$  with respect to an adversary Eve is typically certified by bounding the capacity of

this adversary of guessing  $b$ . Here, we look at a semi-DI prepare-and-measure scenario with untrusted measurements and  $b$  as measurement outcomes. Considering that Eve has bounded knowledge and control over the setup used to generate  $b$ , one can find certifiable bounds on Eve’s guessing probability  $p_g$  which can be used to compute the min-entropy  $H_{min} = -\log_2(p_g)$  [46] of the measurement record. While the single-round min-entropy has served as a benchmark quantifier of randomness, it has been shown that one can bound the min-entropy of a sequence of outcomes in terms of the single-round Shannon entropy instead if the experiment runs over a large number of rounds [47]. This provides more randomness but the statement is valid only under the unrealistic assumption that all rounds are independent and identically distributed (i.i.d.). However, it has recently been shown that one can circumvent the i.i.d. limitation using the so-called Entropy Accumulation Theorem (EAT) generalised to prepare-and-measure scenarios [48, 49].

In this work, we demonstrate a simple semi-DI QRNG to showcase the power of the EAT in prepare-and-measure scenarios. Our protocol is able to certify more than one bit of randomness per round from measurements on a single quantum state. We implement the scheme in a setup using time-bin encoded states and single-photon detection. The protocol employs a prepare-and-measure setup with three states and a single three-outcome measurement. The scheme is semi-DI in the sense that the only assumption on the source is a bound on the pairwise overlap of the prepared states, and the measurement is completely uncharacterised. Randomness is extracted from one of the inputs, and the amount of certified randomness achievable with the generalized EAT is compared with the traditional min-entropy approach. The other two inputs enable self-testing the device, by exploiting that the setup can also be interpreted in terms of a state discrimination task.

In quantum state discrimination [50–52], a measurement device aims to determine which state out of a known set was prepared, subject to certain constraints. In unambiguous state discrimination (USD) [53–55], the error rate is nullified, at the cost of adopting an addi-

\* carles.roch.i.carceller@teorfys.lu.se

† jonatan.brask@fysisk.dtu.dk

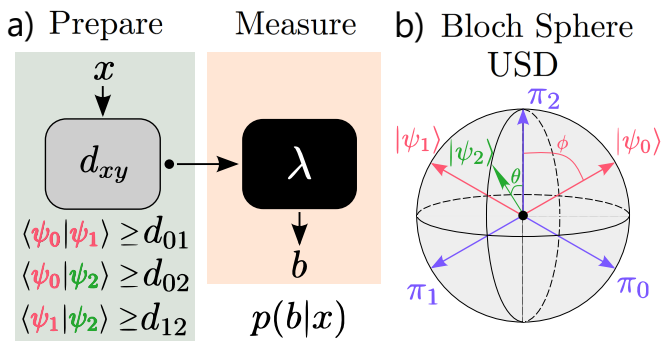


FIG. 1. **a)** Sketch of the semi-device independent prepare-and-measure scenario with three preparations and one untrusted measurement (black box). **b)** The USD protocol is illustrated on the Bloch sphere, with Bloch vectors corresponding to the prepared states  $|\psi_x\rangle$  (red and green) and POVM elements  $\pi_b$  (blue).

tional measurement event which gives no information on which state was prepared (formally called an inconclusive event). The minimum attainable rate of inconclusive events in USD is given by a rank-1 (hence extremal) and unique measurement, which greatly benefits the amount of certifiable randomness on the measurement outcome. Here, we implement a protocol which uses USD during the self-test rounds as in [35], allowing us to make use of the additional inconclusive event in two-state discrimination to reach randomness values greater than one bit per round. Then, we choose a third state that yields equiprobable outcomes when involved in the state discrimination scenario.

The remainder of the paper is organised as follows. In Sec. II, we introduce the state discrimination scenario and specify the measurement strategy. Later, we explain how we evaluate the randomness, continue with the main semi-device independent assumptions we consider and explain how we deal with finite size effects assuming independent and identically distributed (i.i.d.) and non-i.i.d. rounds. We end the section by experimentally implementing the protocol in an optical platform using coherent states of light and present the results we observe both in the experiment and in simulations. In Sec. III we conclude our work, outlining the main result. We end the paper detailing some important particularities involved in the experimental implementation in Sec. IV.

## II. RESULTS

### A. Prepare-and-measure

In order to illustrate the main idea of the protocol, consider the scenario in Fig. 1a, where one party (namely Alice) owns a device that receives inputs  $x \in \{0, 1, 2\}$  with prior probabilities  $p_x$  and prepares the following

pure quantum states,

$$\begin{aligned} |\psi_0\rangle &= \cos \frac{\phi}{2} |0\rangle + \sin \frac{\phi}{2} |1\rangle \\ |\psi_1\rangle &= \cos \frac{\phi}{2} |0\rangle - \sin \frac{\phi}{2} |1\rangle, \end{aligned} \quad (1)$$

and a third qubit state  $|\psi_2\rangle$  which shall remain unspecified for now. These states are sent to a second party (namely Bob) who owns a device which will perform a measurement described by the POVM  $\{\pi_b\}$  for  $b \in \{0, 1, 2\}$ . Over many rounds of the experiment, one can estimate the conditional probability distribution  $p(b|x) = \text{Tr}[\rho_x \pi_b]$ , for  $\rho_x = |\psi_x\rangle \langle \psi_x|$ .

Our first task is to find Bob's optimal measurement, according to a particular state discrimination protocol, to identify whether Alice prepared  $x = 0$  or  $x = 1$ , ignoring the third possible input  $x = 2$ . This will yield correlations reproducible only with extremal and unique POVMs. Then, the idea is to properly design a state  $|\psi_2\rangle$  such that, with that optimal measurement, all outcomes are equiprobable whenever that state is prepared (i.e.  $p(b|x = 2)$  are equal  $\forall b$ ). In order to do that, we take USD as our target strategy.

### B. Unambiguous State Discrimination

The task in USD is to identify which state was prepared without making any errors, i.e.  $p_{\text{error}} := p_0 p(1|0) + p_1 p(0|1) = 0$  [53–55]. That can be done if one pays the price of having some rounds in which the measurement result turns inconclusive. In the present case, USD targets preparations  $x = 0$  and  $x = 1$ , and the inconclusive events will be labeled with  $b = 2$ . The goal of USD is to minimize the rate of inconclusive events  $p_{\text{inc}} := p_0 p(2|0) + p_1 p(2|1)$ . In two state discrimination, the minimum  $p_{\text{inc}}$  is proportional to the overlap of the prepared states, which in our scenario is  $|\langle \psi_0 | \psi_1 \rangle| = \cos \phi$ , according to (1). In this case, the minimum  $p_{\text{inc}}$  is lower bounded by [56]

$$p_{\text{inc}} \geq 2\sqrt{p_0 p_1} \cos \phi. \quad (2)$$

The POVM that represents an optimal USD measurement must be given by rank-1 POVM elements, proportional to the projectors onto the orthogonal states of  $|\psi_0\rangle$  and  $|\psi_1\rangle$ . Concretely, for equiprobable preparations  $p_0 = p_1 = 1/2$ ,

$$\begin{aligned} \pi_0 &= \frac{1}{1 + \cos \phi} |\psi_1^\perp\rangle \langle \psi_1^\perp| \\ \pi_1 &= \frac{1}{1 + \cos \phi} |\psi_0^\perp\rangle \langle \psi_0^\perp| \\ \pi_2 &= \mathbb{1} - \pi_0 - \pi_1, \end{aligned} \quad (3)$$

where  $\langle \psi_x | \psi_x^\perp \rangle = 0$ . Consider now a third preparation  $x = 2$ . We aim to find a state  $|\psi_2\rangle$  which triggers all three outcomes  $b = 0, 1, 2$  of the measurement in (3)

with the same probability. That means, it must satisfy  $\langle \psi_2 | \pi_b | \psi_2 \rangle = 1/3 \forall b$ . As illustrated on the Bloch sphere in Fig. 1b, a good candidate is the state

$$|\psi_2\rangle = \cos \frac{\theta}{2} |0\rangle + i \sin \frac{\theta}{2} |1\rangle . \quad (4)$$

The three outcomes will be equiprobable when

$$\cos \theta = \frac{1 - 2 \cos \phi}{3 \cos \phi} . \quad (5)$$

Since  $-1 \leq \cos \theta \leq 1$ , this condition can only be satisfied for  $\cos \phi \geq 1/5$ , meaning that equiprobable outcomes in this setting are only achievable in that range. One can then use these equiprobable outcomes, which are only reproducible through a unique and extremal POVM in a qubit space, to greatly improve the randomness certification. Note, though, that this is only true for qubit states. In semi-DI randomness certification, one wants to keep the number of assumptions at minimum. We will later show how we can get rid of the assumption of a fixed dimension.

### C. Randomness certification

We proceed to explain how we certify randomness in the measurement outcomes, relative to an adversary Eve. Eve has knowledge of the preparation ( $x$ ) and measurement device, and can share classical correlations with the measurement according to the distribution  $q(\lambda)$ . We begin explaining how we certify single-round randomness using the min-entropy. Then, we leverage the power of the EAT to accommodate the finite-size effect from experimental data and bound the Shannon entropy.

**Min-entropy:** We certify randomness only from rounds where state  $|\psi_2\rangle$  is prepared. The rounds where states  $|\psi_0\rangle$  and  $|\psi_1\rangle$  are prepared can be thought of as self-test rounds. During the rounds where  $|\psi_2\rangle$  is prepared, Eve's guessing probability averaged through each round can be written as

$$p_g = \sum_{\lambda} q(\lambda) \max_b \{p(b|x=2, \lambda)\} , \quad (6)$$

for  $p(b|x, \lambda) = \text{Tr} [\rho_x \pi_b^\lambda]$  ( $\rho_x = |\psi_x\rangle \langle \psi_x|$ ) being the probability that the measurement outcome is  $b$  given state preparation  $x$  and the measurement strategy  $\lambda$ .

We aim to find an upper bound on  $p_g$  in (6) over all strategies of Eve, i.e. all distributions  $q(\lambda)$  and measurements  $\pi_b^\lambda$ , subject to reproducing the observed statistics on average  $p(b|x) = \sum_{\lambda} q(\lambda) \text{Tr} [\rho_x \pi_b^\lambda]$ . This optimisation problem can be rendered as a semi-definite program (SDP) [57]. As we detail in App. A, we can write Eve's guessing probability as

$$p_g = \sum_{\lambda} \text{Tr} [\rho_2 M_b^\lambda] . \quad (7)$$

An upper bound  $p_g^* \geq p_g$  can be found by maximizing (7) over all positive semidefinite  $D \times D$  matrices  $M_b^\lambda$  that fulfil the constraints

$$\sum_b M_b^\lambda = \frac{1}{D} \text{Tr} \left[ \sum_b M_b^\lambda \right] \mathbf{1} \quad \forall \lambda , \quad (8)$$

$$p(b|x) = \sum_{\lambda} \text{Tr} [M_b^\lambda \rho_x] \quad \forall b, x . \quad (9)$$

where  $D$  is the eavesdropper's dimension. The randomness of the measurement outcomes is quantified through the min-entropy  $H_{\min} = -\log_2(p_g)$ , which gives the number of (almost) uniformly random bits which can be extracted per round of the protocol [46].

**Shannon entropy:** Due to the non-linear nature of the Shannon entropy, it is very difficult to find linear schemes that provide tight numerical bounds in single-party prepare-and-measure scenarios. For example, in Ref. [39] the authors design a hierarchy of SDPs to bound the Shannon entropy in scenarios with energy-restricted correlations. Here, our correlations are bounded by a constraint on the overlaps and thus, we find the following method more suitable. As shown in Ref. [58], applying the Gauss-Radau quadrature to an integral representation of the logarithm yields a variational upper bound for the quantum relative entropy  $D(\rho||\sigma) := \text{Tr} [\rho (\log \rho - \log \sigma)]$ . This can be related to the Von Neumann entropy, and consequently to the Shannon entropy for classically correlated eavesdroppers. In App. B we show how to use this technique to derive the following bound on the Shannon entropy,

$$S \geq S^* := \sum_{i,b,\lambda} \tau_i q(\lambda) f_{i,x=2}^{\lambda b} , \quad (10)$$

for

$$f_{i,x}^{\lambda b} = \inf_{z_i^{\lambda b}, \eta_i^{\lambda b}} \{1 + p(b|x, \lambda) (2z_i^{\lambda b} + (1 - t_i)\eta_i^{\lambda b}) + t_i \eta_i^{\lambda b}\} ,$$

where we introduced  $\tau_i := \omega_i / (t_i \log(2))$  for  $\{t_i, \omega_i\}$  being the nodes and weights respectively, corresponding to the Gauss-Radau quadrature. The right-hand side in (10) should be minimised over strategies of Eve. This can be done through a series of SDPs operating in a *see-saw* manner. That is, alternate the optimisation over the arbitrary scalars  $\{z_i^{\lambda b}, \eta_i^{\lambda b}\}$  for fixed probability distributions  $\{q(\lambda), p(b|x, \lambda)\}$  with the constraint

$$\begin{pmatrix} 1 & z_i^{\lambda b} \\ z_i^{\lambda b} & \eta_i^{\lambda b} \end{pmatrix} \geq 0 , \quad (11)$$

and the optimisation over  $D \times D$  positive semidefinite matrices  $M_b^\lambda$  that fulfil the constraints in (8) and (9). We let the see-saw optimisation run over a limited number of rounds  $n$  and store the average difference between solutions in consecutive rounds, i.e.  $\Delta_k := \sum_{r=n(1+k)}^{nk} |S_r^* - S_{r+1}^*| / n$ , for  $k = 0, 1, 2, \dots$ . The process is repeated as long as  $\Delta_k \geq 10^{-4}$  or unless a critical

$k$  is reached, at which point the algorithm is re-started with an alternative random point.

We note that the *see-saw* approach is not guaranteed, in principle, to attain a global minimum and thus generally provides only an upper bound on the minimum of the right-hand side in (10), while what we need is a lower bound. However, we have tested extensively that the minimisation provides stable results under changes to initial conditions and stopping criteria. Furthermore, preliminary comparison to new methods under preparation [59], that provide true lower bounds, show that the *see-saw* does attain the true minimum in our case.

#### D. Semi-DI characterization

We do not wish to assume the prepared states above to be completely characterised, nor do we wish to assume that the dimension of Eve's system is known. Instead, we will assume only knowledge about the overlaps (non-orthogonality) between the states. For two preparations, this allows using two fixed qubit states in the SDP without loss of generality, because unitary rotations of the state pair will not affect the optimum, and Eve will not gain any extra information by extending the measurements beyond the two-dimensional span of the pair [38]. In our case we consider three states, which means that Eve's maximal useful dimensionality will not exceed a qutrit space. Hence, we need to assume that the three prepared states span a three-dimensional space. That is, the third state is

$$|\tilde{\psi}_2\rangle = \sqrt{a}|\psi_2\rangle + \sqrt{1-a}|2\rangle, \quad (12)$$

for  $|\psi_2\rangle$  in (4) having support on the bi-dimensional space spanned by  $|\psi_0\rangle$  and  $|\psi_1\rangle$  in (1), and  $|2\rangle$  has only support on an additional orthogonal dimension, such that  $\langle\psi_x|2\rangle = 0 \forall x$ . One can see that, if both overlaps  $|\langle\tilde{\psi}_2|\psi_0\rangle|^2$  and  $|\langle\tilde{\psi}_2|\psi_1\rangle|^2$  are simultaneously fixed to be

$$|\langle\tilde{\psi}_2|\psi_0\rangle|^2 = |\langle\tilde{\psi}_2|\psi_1\rangle|^2 = \frac{1}{2}(1 + \cos\phi\cos\theta), \quad (13)$$

then the normalisation in (12) imposes  $a = 1$ , and all three preparations must have support on a qubit space. However, strict equalities can be hard to satisfy in the lab. In App. C we show how one can relax this assumption to lower bounds on the overlaps  $|\langle\psi_x|\psi_y\rangle| \geq d_{xy}$ . This, in turn, bounds the access of the eavesdropper to an additional third dimension, as  $a$  fulfills

$$a \geq \frac{d_{02}^2 + d_{12}^2 - 2d_{01}d_{02}d_{12}}{1 - d_{01}^2}. \quad (14)$$

Also, since  $a \leq 1$ , one also finds the following relation

$$1 \geq d_{02}^2 + d_{12}^2 + d_{01}^2 - 2d_{01}d_{02}d_{12}, \quad (15)$$

which must hold true for any dimension. Equation (14) defines the surface of an inflated tetrahedron with curved

faces (see App. C). The amplitude  $a$  decreases towards the center of the tetrahedron. Thus, in other words, bounding  $|\langle\psi_x|\psi_y\rangle| \geq d_{xy}$  implies that we forbid Eve to access the interior of the tetrahedron.

This semi-DI characterisation allows us to compute the certifiable randomness beyond the two-qubit case and avoid direct dimensional constraints. In our implementation, we employ coherent states of light. We control the pairwise overlaps of the preparation and use (14) to bound their support outside a two-dimensional subspace.

#### E. Finite-size effects – i.i.d. vs. entropy accumulation

In actual experiments, probabilities are estimated from frequencies. Due to the finite number of data points, the observed frequency of events  $\text{freq.}(b|x) = n_{bx}/n_x$ , for  $n_{bx}$  denoting the total number of events  $b$  given a state preparation  $x$  does not exactly represent the true conditional probability  $p(b|x)$ . To deal with finite-size effects, we take two different approaches.

First, we assume that all rounds from the experiment are considered to be independent and identically distributed (i.i.d.). Under this assumption, we recall the asymptotic equitation property (AEP). The AEP establishes that the output of a random experiment is certain to come from the typical set, under the limit of large number of repetitions. In Ref. [47] a generalisation of the AEP to quantum theory is developed, establishing that the *smooth min-entropy*  $H_{\min}^\varepsilon$  (i.e. the maximum min-entropy for any state  $\varepsilon$ -close to a fixed state [60]) converges to the conditional Von Neumann entropy up to an error term. Our case simplifies this statement to the Shannon entropy, because only classical side information is considered here. Specifically,

$$\frac{1}{N}H_{\min}^\varepsilon(B^N|E^N, x=2) \geq S^* - \frac{\delta}{\sqrt{N}}, \quad (16)$$

for  $H_{\min}^\varepsilon(B^N|E^N, x=2)$  being the smooth min-entropy accumulated over a total of  $N$  experimental rounds for a particular preparation  $x=2$ , and  $\delta$  a parameter defined in App. E. By  $S^*$  we denoted a lower-bound on the single-round Shannon entropy assuming i.i.d., which can be estimated from the see-saw optimisation of Sec. II C

Next, we go beyond the i.i.d. assumption and perform a second characterization of finite size effects. In this case, we use the entropy accumulation theorem (EAT) generalised to prepare-and-measure scenarios [48, 49], which allows us to quantify the amount of entropy accumulated per round also when they are not i.i.d. The EAT places a bound on the conditional smooth min-entropy, which depends only on the Von Neumann entropy per round plus a correction term which depends on the total number of rounds in the experiment. Every round of the experiment is described by a channel  $\mathcal{M}_i$  which maps Bob's ( $B_i$ ) and Eve's ( $E_i$ ) systems to their corresponding systems in the next round ( $B_{i+1}$  and  $E_{i+1}$  respectively). To

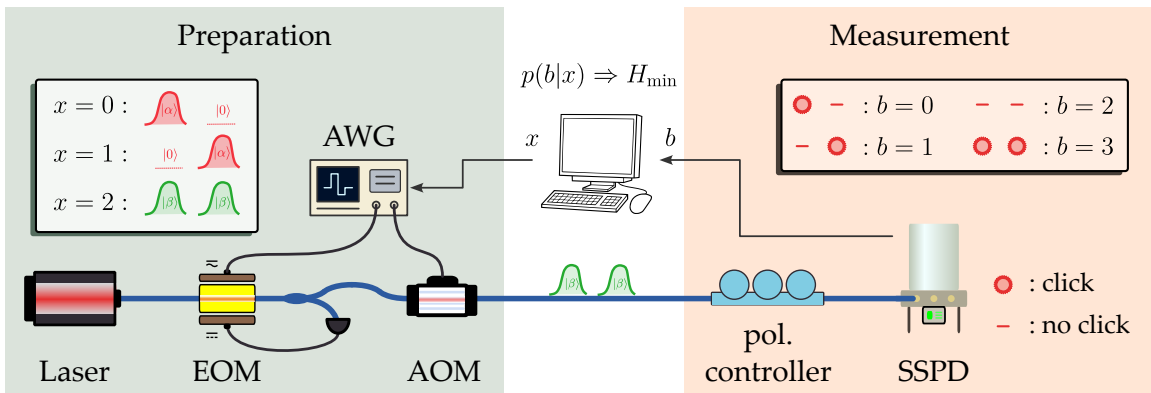


FIG. 2. Experimental implementation. The time-bin-encoded input states are generated by an electro-optic modulator (EOM) and an acousto-optic modulator (AOM). The feedback control at the EOM stabilizes the amplitude of the pulsed weak coherent states. After optimizing the polarization (pol. controller), the pulses are sent to the superconducting single-photon detector (SSPD). From the statistics of preparations and detector counts, randomness is extracted and certified.

make the EAT applicable in our experiment, we assume a no-signaling constraint between Bob and Eve’s devices. The marginal of the new side information  $E_i$  without the new output  $B_i$  must be reproducible only with past side information  $E_{i-1}$  (i.e. any new  $E_i$  should depend on past  $E_{i-1}$  alone). This forbids that Eve’s information  $E_i$  is passed along Bob’s systems  $B_{i-1}$ , which would mean that, in some cases,  $E_{i-1}$  holds no information on Bob’s outcome but  $E_i$  does. In App. E we explain in more detail how we apply the EAT to our results to certify the randomness outside the i.i.d. assumption. Concretely, we are able to bound the smooth-min-entropy on the measurement outcome using the single-round Shannon entropy plus a correction term, i.e.

$$\frac{1}{N} H_{\min}^{\varepsilon}(B^N | E^N, x = 2) \geq S^* - \mathcal{O}(1/\sqrt{N}), \quad (17)$$

where again  $S^*$  is a lower bound on the i.i.d. Shannon entropy and can be estimated from the see-saw optimization of Sec. II C.

Finally, to extract the randomness from the whole sequence of Bob’s outcomes, we use a randomness extractor. Here we shortly introduce the meaning of this function and the main result we use in this work. For a more detailed explanation refer to Ref. [49]. Consider  $H_{\min}^{\varepsilon}(B^N | E^N) \geq h$ . A quantum-proof strong  $(h, \varepsilon_{\text{EXT}})$ -extractor is defined as a function EXT that receives a quantum state  $\rho_{BE} \otimes \tau_S$  and acts on the classical systems  $B$  and  $S$  with dimension equal to  $n_B \times n_S$  bits. The  $l$ -bit dimensional output  $\text{EXT}(\rho_{BE} \otimes \tau_S)$  is  $\tilde{\varepsilon}_{\text{EXT}}$ -close to  $\tau_L \otimes \rho_E \otimes \tau_S$ . Here  $\tau_L$  and  $\tau_S$  are maximally mixed states of dimension  $2^{n_S}$  and  $2^l$ , and  $\rho_{BE}$  is the classical-quantum state shared by Bob and Eve after the measurement. The input in system  $S$  is called the seed of the extractor. The security parameter of this extractor is given by  $\tilde{\varepsilon}_{\text{EXT}} := \varepsilon_{\text{EXT}} + 4\varepsilon$ , which can be arbitrarily chosen. Furthermore, there exists a quantum-proof strong

$(h, \varepsilon_{\text{EXT}})$ -extractor from which we can extract a total of  $l \leq h - 2 \log_2(1/\varepsilon_{\text{EXT}})$  random bits [60]. In all results from this work we consider  $\varepsilon_{\text{EXT}} = 10^{-8}$ , which implies an additional correction of  $\sim -26/N$  in the extractable randomness per round.

## F. Implementation

We implement the protocol using time-bin encoded coherent states and single-photon detection. Our approach is inspired by previous works in similar settings [35, 42]. The setup is illustrated in Fig. 2. In the following, we briefly sketch its working principle. In Sec. IV, we provide more detail.

Our photon source is a 1550 nm continuous-wave laser. We use an electro-optic modulator (EOM) and an acousto-optic modulator (AOM) to carve the output of the laser into 10 ns-width pulsed coherent states with appropriate amplitude. In each round, the pulses can emerge in an early or a late time-bin. The two self-testing states for  $x = 0$  and  $x = 1$  are prepared using a coherent state with amplitude  $\alpha$  in the early and late bins, respectively. We write this as  $|\psi_0\rangle = |\alpha 0\rangle$  and  $|\psi_1\rangle = |0\alpha\rangle$ . On the other hand, the third state,  $x = 2$ , used for randomness extraction is prepared using amplitude  $\beta$  in both early and late bins,  $|\psi_2\rangle = |\beta\beta\rangle$ .

The measurement is performed by a superconducting single-photon detector (ID Quantique ID281) with a quantum efficiency of 94% which detects photons from the carved, attenuated laser beam. The outcome  $b$  is determined by in which time bin the detector clicks. We label events with clicks in only the early time-bin by  $b = 0$ , events with clicks only in the late time-bin by  $b = 1$ , events with no clicks in either bin by  $b = 2$ , and events with clicks in both bins by  $b = 3$ . As discussed in App. D, the fourth outcome is binned with the first two. Using

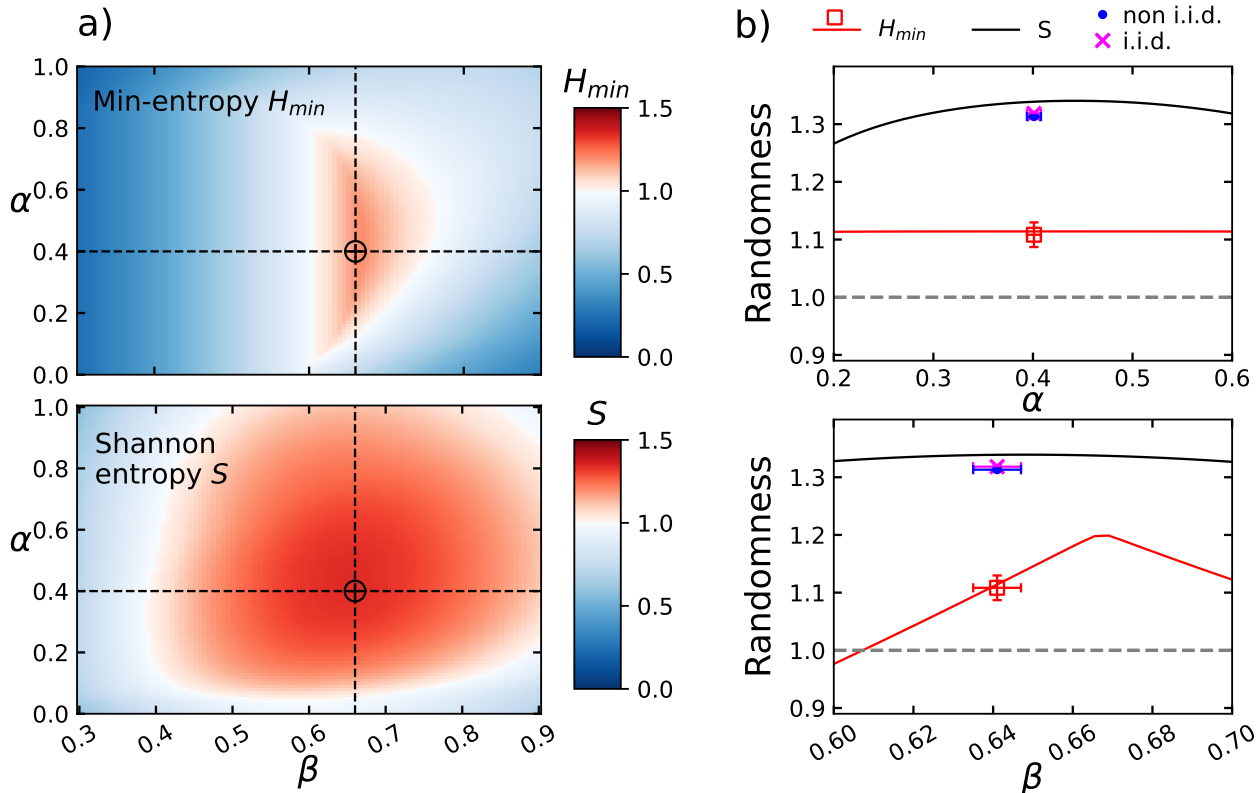


FIG. 3. **a)** Bound on the raw min and Shannon entropies (i.e. without accounting for finite size effects) as a result from the SDPs presented in Sec. II C for a limited range of coherent amplitudes. Red regions denote more than one bit of randomness per round. The targeted amplitudes  $\alpha_T = 0.4$  and  $\beta_T = 0.66$  are denoted with black-dashed lines. **b)** Slice of the color plots at the chosen amplitudes. We compare the raw min-entropy, the Shannon entropy and the certifiable randomness through the AEP (non i.i.d.) and generalised EAT (i.i.d.). The results of the experiment are shown in a cross/circle/square with their corresponding error bars. The chosen parameters are  $m = 8$ ,  $\varepsilon = 10^{-8}$  with photon loss  $1 - \eta = 0.06$ , dark count probability of  $p_{dc} = 10^{-6}$  and total number of samples  $N \simeq 10^7$  over 11 distinct repetitions.

the measurement setup, in a calibration step, we also determine the AOM and EOM voltages required to prepare coherent states  $|\alpha\rangle$  and  $|\beta\rangle$  with the desired overlap.

### G. Simulation and observation

In order to find optimal experimental settings, we first simulate the system, computing the randomness for varying coherent-state amplitudes. In Fig. 3 we show the min-entropy under realistic conditions (including loss and detector dark counts). The results show maximal min-entropy around the amplitudes  $\alpha_T = 0.4$  and  $\beta_T = 0.66$ , which we therefore target in the experiment. This corresponds to states  $|\psi_x\rangle$  with overlaps  $|\langle\psi_0|\psi_1\rangle| = 0.84$  and  $|\langle\psi_0|\psi_2\rangle| = |\langle\psi_1|\psi_2\rangle| = 0.78$ . We note these fulfil the criterion  $|\langle\psi_0|\psi_1\rangle| \geq 1/5$  deduced from (5) for the possibility of equiprobable outcomes. These preparations should thus allow correlations yielding high values of randomness. We additionally run the see-saw optimi-

sation method to efficiently compute direct bounds on the Shannon entropy using the exact same realistic settings. Comparing with the min-entropy results, we find a marked increase in the certifiable randomness, as well as a vast expansion of the usable parameter region. Although the optimal randomness in this case is not exactly given by the targeted amplitudes  $\alpha_T$  and  $\beta_T$ , we keep them to directly compare the best possible certifiable randomness using the min-entropy vs. the Shannon entropy.

The overlaps constrain support outside the span of  $|\psi_0\rangle$  and  $|\psi_1\rangle$  but do not eliminate it. Specifically, the minimal amplitude introduced in (12) is  $a \geq 0.66$  on the targeted coherent amplitudes. Moreover, the conditional probability  $p(b|2)$  does not depend on  $\alpha$ . However, we do see some dependency on  $\alpha$  in the randomness in Fig. 3, which becomes more evident for higher values of  $\beta$ . The fact that  $a < 1$  for our amplitudes is the main responsible of that dependency and also implies that the correlations are not reproducible only by unique and extremal POVMs. This reduces the secrecy of the outcome, decreasing the certifiable randomness. Nevertheless, we are able to find a

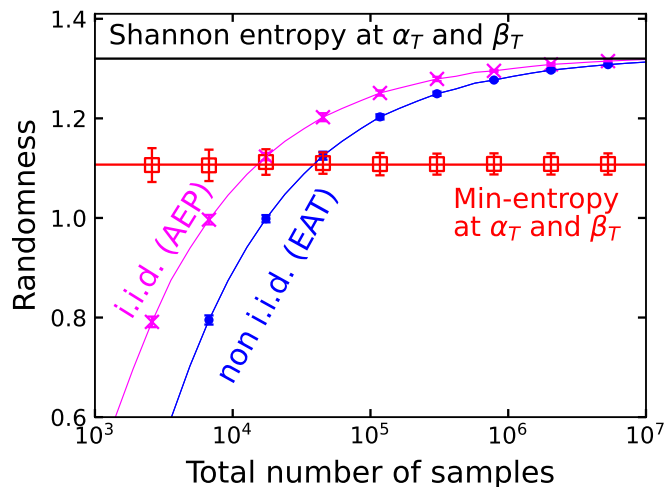


FIG. 4. Scaling of i.i.d. and non i.i.d. bounds with the number of rounds in the experiment. In our experiment we took  $\sim 10^7$  samples, which explains the almost-equivalency between both approaches in our results.

set of amplitudes where, although Eve has unbounded dimensionality, her guessing probability is lower than  $1/2$ , i.e. more than one bit of randomness is certified using the min-entropy and even more with the Shannon entropy.

We run the experiment through the proposed implementation and evaluate the randomness for a single configuration of targeted amplitudes. We show the obtained results in Fig. 3 (right-side plots). The experimental data we collected indicate that the actual amplitudes used in the lab were  $\alpha_L = 0.401 \pm 0.007$  and  $\beta_L = 0.641 \pm 0.006$ . Our observations agree well with the predictions from the simulations, and show a randomness extraction rate of  $1.322 \pm 0.002$  and  $1.319 \pm 0.002$  bits per round after  $10^7$  runs of the experiment, when analysed assuming i.i.d. experiment rounds using the asymptotic equipartition property (AEP) and without i.i.d. rounds using the entropy accumulation theorem (EAT), respectively. Additionally, we compute the raw min-entropy per round without taking into account finite size effects and, using the experimental data, we obtain  $1.11 \pm 0.02$  bits of randomness per round. All error bars (also shown in Fig. 3) are the standard deviation obtained over running the experiment 11 different times. We observe a 19% improvement in the certifiable randomness by using the Shannon entropy (which is computed in the AEP and EAT approaches) compared to the min-entropy. Also, the estimated errors using the AEP and EAT approaches are lower than the min-entropy approach by one order of magnitude. This is mainly because the Shannon entropy is more stable than the min-entropy against fluctuations on the coherent amplitudes. Furthermore, the reason behind the almost-equivalence between the i.i.d. and non i.i.d. value is due to the high amount of samples gathered in the experiment (around  $10^7$ ) which foresees the convergence of the EAT to the AEP in the limit of in-

finite number of experimental rounds. In Fig. 4 we additionally collected random subsets between  $10^3$  and  $10^7$  data-points from the 11 different gathered experimental data-sets and computed the randomness using the raw min-entropy, the i.i.d. (AEP) and non i.i.d. (EAT) approaches. Observe that the total of  $10^7$  experimental rounds lies close to the asymptotic limit. Nevertheless, note that the non i.i.d. approach is still able to certify more randomness than the raw min-entropy down to approximately  $3.8 \times 10^4$  samples.

### III. DISCUSSION

We have realized a semi-DI randomness generation protocol implemented in an optical platform, as shown in Fig. 2. By exploiting the entropy accumulation theorem generalised to prepare-and-measure scenarios, we bound the certifiable randomness in terms of the single-round Shannon entropy without assuming that experimental rounds are independent and identically distributed (i.i.d.) and including finite-size effects. We show that this allows certifying significantly more randomness than a standard approach bounding the single-round min-entropy under an i.i.d. assumption and neglecting finite-size effects. Thus, we certify more randomness under much less restrictive assumptions.

### IV. METHODS

As sketched in the main text, the input states used in the experiment are created by using an EOM capable of inducing intensity modulation, and a sequence of two AOMs to carve the output of a 1550.32 nm continuous-wave laser into time-bin-encoded series of pulsed weak coherent states. Concretely, the AOMs attenuate the output of the laser by 77 dB when sending a pulse, so the intensities of the output states are at a single-photon level, and it completely shuts off the laser output when no pulse is being sent. In doing so, we achieve a dark count rate of only  $p_{dc} = (4.5 \pm 2.8) \times 10^{-6}$  per pulse. The EOM, on the other hand, generates the correct amplitudes for the input states during a 10 ns time window, which is chosen as the duration of the time-bin. The early and late pulses are separated by 800 ns and the full protocol runs at a 0.526 MHz rate. To ensure high efficiency of the photodetection, we optimize the polarization state of the photons with a fiber polarization controller before the superconducting detector and splice all the fiber connection points in the measurement stage to minimize the photon loss.

The values for  $\alpha$  and  $\beta$  are calibrated using a single-photon detector with a specified efficiency of  $\eta = 94\%$ . Based on the amplitude we desire to achieve, we are able to calculate the click rate related to this coherent state. Further, we have introduced a feedback control loop to stabilize the output power of the EOM to stabilize the

coherent state amplitudes throughout the experiment. From the measured counting rates, we deduce the coherent state amplitude we sent to be  $\alpha_L = 0.401 \pm 0.007$  and  $\beta_L = 0.641 \pm 0.006$ . Here, the  $1\sigma$  standard deviations are caused by the residual intensity fluctuations across the data collection time of the entire experiment.

In order to reduce finite size effects, we take around  $10^8$  rounds of measurements. After gathering every  $10^7$  round of data, we perform a calibration measurement before taking the data again. The fluctuation of the count rate, measured by the standard deviation across all experiment runs, is only 1.52% relative to the average value, certifying the consistency between the states prepared at

different times.

## ACKNOWLEDGMENTS

C.R.C. is supported by the Wenner-Gren Foundation. We gratefully acknowledge support from the Danish National Research Foundation, Center for Macroscopic Quantum States (bigQ, DNRF142), VILLUM FONDEN (research grant 40864), the Carlsberg Foundation CF19-0313, Innovation Fund Denmark (PhotoQ project, grant no. 1063-00046A), the Horizon Europe MSCA (Project GTGBS, grant no. 101106833) and a DTU-KAIST Alliance Stipend.

- 
- [1] B. Hayes, Randomness as a resource, *American Scientist* **89**, 300 (2001).
- [2] C. E. Shannon, Communication theory of secrecy systems, *The Bell System Technical Journal* **28**, 656 (1949).
- [3] B. S. Niels Ferguson and T. Kohno, *Cryptography engineering: design principles and practical applications* (John Wiley and Sons, 2011).
- [4] N. Metropolis and S. Ulam, The monte carlo method, *Journal of the American Statistical Association* **44**, 335 (1949), pMID: 18139350.
- [5] N. Metropolis, A. W. Rosenbluth, M. N. Rosenbluth, A. H. Teller, and E. Teller, Equation of state calculations by fast computing machines, *J. Chem. Phys.* **21**, 1087 (1953).
- [6] A. Montanaro, Quantum speedup of monte carlo methods, *Proc. R. Soc. A.* **471**, 10.1098/rspa.2015.0301 (2015).
- [7] D. Ghersi, A. Parakh, and M. Mezei, Comparison of a quantum random number generator with pseudorandom number generators for their use in molecular monte carlo simulations, *Journal of Computational Chemistry* **38**, 2713 (2017), <https://onlinelibrary.wiley.com/doi/pdf/10.1002/jcc.25065>.
- [8] K. Miyamoto and K. Shiohara, Reduction of qubits in a quantum algorithm for monte carlo simulation by a pseudo-random-number generator, *Phys. Rev. A* **102**, 022424 (2020).
- [9] F. James, A review of pseudorandom number generators, *Computer Physics Communications* **60**, 329 (1990).
- [10] X. Ma, X. Yuan, Z. Cao, B. Qi, and Z. Zhang, Quantum random number generation, *npj Quantum Information* **2**, 16021 (2016).
- [11] M. Herrero-Collantes and J. C. Garcia-Escartin, Quantum random number generators, *Rev. Mod. Phys.* **89**, 015004 (2017).
- [12] M. N. Bera, A. Acín, M. Kuś, M. W. Mitchell, and M. Lewenstein, Randomness in quantum mechanics: philosophy, physics and technology, *Reports on Progress in Physics* **80**, 124001 (2017).
- [13] P. Grangier and A. Auffèves, (*Phil. Trans. R. Soc. A.*, 2018).
- [14] N. Brunner, D. Cavalcanti, S. Pironio, V. Scarani, and S. Wehner, Bell nonlocality, *Rev. Mod. Phys.* **86**, 419 (2014).
- [15] R. Colbeck, Quantum and relativistic protocols for secure multi-party computation, Ph.D. Thesis, University of Cambridge (2009), arXiv:0911.3814 [quant-ph].
- [16] S. Pironio, A. Acín, A. Massar, S. and Boyer de la Giroday, D. N. Matsukevich, P. Maunz, S. Olmschenk, D. Hayes, L. Luo, T. A. Manning, and C. Monroe, Random numbers certified by bell's theorem, *Nature* **464**, 1021 (2010).
- [17] A. Acín and L. Masanes, Certified randomness in quantum physics, *Nature* **540**, 213 (2016).
- [18] B. G. Christensen, K. T. McCusker, J. B. Altepeter, B. Calkins, T. Gerrits, A. E. Lita, A. Miller, L. K. Shalm, Y. Zhang, S. W. Nam, N. Brunner, C. C. W. Lim, N. Gisin, and P. G. Kwiat, Detection-loophole-free test of quantum nonlocality, and applications, *Phys. Rev. Lett.* **111**, 130406 (2013).
- [19] Y. Liu, Q. Zhao, M.-H. Li, J.-Y. Guan, Y. Zhang, B. Bai, W. Zhang, W.-Z. Liu, C. Wu, X. Yuan, H. Li, W. J. Munro, Z. Wang, L. You, J. Zhang, X. Ma, J. Fan, Q. Zhang, and J.-W. Pan, Device-independent quantum random-number generation, *Nature* **562**, 548 (2018).
- [20] P. Bierhorst, E. Knill, S. Glancy, Y. Zhang, A. Mink, S. Jordan, A. Rommal, Y.-K. Liu, B. Christensen, S. W. Nam, M. J. Stevens, and L. K. Shalm, Experimentally Generated Randomness Certified by the Impossibility of Superluminal Signals, *Nature* **556**, 223 (2018).
- [21] L. K. Shalm, Y. Zhang, J. C. Bienfang, C. Schlager, M. J. Stevens, M. D. Mazurek, C. Abellán, W. Amaya, M. W. Mitchell, M. A. Alhejji, H. Fu, J. Ornstein, R. P. Mirin, S. W. Nam, and E. Knill, Device-independent randomness expansion with entangled photons, *Nature Physics* **17**, 452 (2021).
- [22] W.-Z. Liu, M.-H. Li, S. Ragy, S.-R. Zhao, B. Bai, Y. Liu, P. J. Brown, J. Zhang, R. Colbeck, J. Fan, Q. Zhang, and J.-W. Pan, Device-independent randomness expansion against quantum side information, *Nature Physics* **17**, 448 (2021).
- [23] H.-W. Li, Z.-Q. Yin, Y.-C. Wu, X.-B. Zou, S. Wang, W. Chen, G.-C. Guo, and Z.-F. Han, Semi-device-independent random-number expansion without entanglement, *Phys. Rev. A* **84**, 034301 (2011).
- [24] G. Vallone, D. G. Marangon, M. Tomasin, and P. Villoresi, Quantum randomness certified by the uncertainty principle, *Phys. Rev. A* **90**, 052327 (2014).



- [25] E. Passaro, D. Cavalcanti, P. Skrzypczyk, and A. Acín, Optimal randomness certification in the quantum steering and prepare-and-measure scenarios, *New Journal of Physics* **17**, 113010 (2015).
- [26] T. Lunghi, J. B. Brask, C. C. W. Lim, Q. Lavigne, J. Bowles, A. Martin, H. Zbinden, and N. Brunner, Self-testing quantum random number generator, *Phys. Rev. Lett.* **114**, 150501 (2015).
- [27] A. Chaturvedi and M. Banik, Measurement-device-independent randomness from local entangled states, *EPL (Europhysics Letters)* **112**, 30003 (2015).
- [28] Z. Cao, H. Zhou, and X. Ma, Loss-tolerant measurement-device-independent quantum random number generation, *New J. Phys.* **17**, 125011 (2015).
- [29] Y.-Q. Nie, J.-Y. Guan, H. Zhou, Q. Zhang, X. Ma, J. Zhang, and J.-W. Pan, Experimental measurement-device-independent quantum random-number generation, *Phys. Rev. A* **94**, 060301 (2016).
- [30] Z. Cao, H. Zhou, X. Yuan, and X. Ma, Source-Independent Quantum Random Number Generation, *Phys. Rev. X* **6**, 011020 (2016).
- [31] F. Xu, J. H. Shapiro, and F. N. C. Wong, Experimental fast quantum random number generation using high-dimensional entanglement with entropy monitoring, *Optica* **3**, 1266 (2016).
- [32] F. Bischof, H. Kampermann, and D. Bruß, Measurement-device-independent randomness generation with arbitrary quantum states, *Phys. Rev. A* **95**, 062305 (2017).
- [33] D. G. Marangon, G. Vallone, and P. Villoresi, Source-device-independent ultrafast quantum random number generation, *Phys. Rev. Lett.* **118**, 060503 (2017).
- [34] T. Van Himbeek, E. Woodhead, N. J. Cerf, R. García-Patrón, and S. Pironio, Semi-device-independent framework based on natural physical assumptions, *Quantum* **1**, 33 (2017).
- [35] J. B. Brask, A. Martin, W. Esposito, R. Houlmann, J. Bowles, H. Zbinden, and N. Brunner, Megahertz-Rate Semi-Device-Independent Quantum Random Number Generators Based on Unambiguous State Discrimination, *Phys. Rev. Appl.* **7**, 054018 (2017).
- [36] M. Avesani, D. G. Marangon, G. Vallone, and P. Villoresi, Source-device-independent heterodyne-based quantum random number generator at 17 gbps, *Nature Communications* **9**, 5365 (2018).
- [37] T. Michel, J. Y. Haw, D. G. Marangon, O. Thearle, G. Vallone, P. Villoresi, P. K. Lam, and S. M. Assad, Real-time source-independent quantum random-number generator with squeezed states, *Phys. Rev. Applied* **12**, 034017 (2019).
- [38] D. Rusca, T. van Himbeek, A. Martin, J. B. Brask, W. Shi, S. Pironio, N. Brunner, and H. Zbinden, Self-testing quantum random-number generator based on an energy bound, *Phys. Rev. A* **100**, 062338 (2019).
- [39] T. V. Himbeek and S. Pironio, Correlations and randomness generation based on energy constraints (2019), arXiv:1905.09117 [quant-ph].
- [40] D. Drahi, N. Walk, M. J. Hoban, A. K. Fedorov, R. Shakhovoy, A. Feimov, Y. Kurochkin, W. S. Kolthammer, J. Nunn, J. Barrett, and I. A. Walmsley, Certified quantum random numbers from untrusted light, *Phys. Rev. X* **10**, 041048 (2020).
- [41] M. Pivoluska, M. Plesch, M. Farkas, N. Ružičková, C. Flegel, N. H. Valencia, W. McCutcheon, M. Malik, and E. A. Aguilar, Semi-device-independent random number generation with flexible assumptions, *npj Quantum Information* **7**, 50 (2021).
- [42] H. Tebyanian, M. Zahidy, M. Avesani, A. Stanco, P. Villoresi, and G. Vallone, Semi-device independent randomness generation based on quantum state's indistinguishability, *Quantum Science and Technology* **6**, 045026 (2021).
- [43] C. Wang, I. W. Primaatmaja, H. J. Ng, J. Y. Haw, R. Ho, J. Zhang, G. Zhang, and C. Lim, Provably-secure quantum randomness expansion with uncharacterised homodyne detection, *Nature Communications* **14**, 316 (2023).
- [44] J. Argillander, A. Alarcón, C. Bao, C. Kuang, G. Lima, F. Gao, and G. B. Xavier, Quantum random number generation based on a perovskite light emitting diode, *Communications Physics* **6**, 157 (2023).
- [45] P. Mironowicz, G. Cañas, J. Cariñe, E. S. Gómez, J. F. Barra, A. Cabello, G. B. Xavier, G. Lima, and M. Pawłowski, Quantum randomness protected against detection loophole attacks (2021).
- [46] R. König, R. Renner, and C. Schaffner, The operational meaning of min- and max-entropy, *IEEE Transactions on Information Theory* **55**, 4337 (2009).
- [47] M. Tomamichel, R. Colbeck, and R. Renner, A fully quantum asymptotic equipartition property, *IEEE Transactions on Information Theory* **55**, 5840 (2009).
- [48] T. Metger, O. Fawzi, D. Sutter, and R. Renner, Generalised entropy accumulation, in *2022 IEEE 63rd Annual Symposium on Foundations of Computer Science (FOCS)* (2022) pp. 844–850.
- [49] T. Metger and R. Renner, Security of quantum key distribution from generalised entropy accumulation, *Nature Communications* **14**, 5272 (2023).
- [50] J. A. Bergou, Quantum state discrimination and selected applications, *Journal of Physics: Conference Series* **84**, 012001 (2007).
- [51] S. M. Barnett and S. Croke, Quantum state discrimination, *Adv. Opt. Photon.* **1**, 238 (2009).
- [52] J. Bae and L.-C. Kwek, Quantum state discrimination and its applications, *Journal of Physics A: Mathematical and Theoretical* **48**, 083001 (2015).
- [53] I. D. Ivanovic, How to differentiate between non-orthogonal states, *Physics Letters A* **123**, 257 (1987).
- [54] D. Dieks, Overlap and distinguishability of quantum states, *Physics Letters A* **126**, 303 (1988).
- [55] A. Peres, How to differentiate between non-orthogonal states, *Physics Letters A* **128**, 19 (1988).
- [56] C. Roch i Carceller, *Quantum state discrimination with applications in contextuality and randomness certification*, Ph.D. thesis (2023).
- [57] P. Skrzypczyk and D. Cavalcanti, *Semidefinite Programming in Quantum Information Science*, 2053-2563 (IOP Publishing, 2023).
- [58] P. Brown, H. Fawzi, and O. Fawzi, Device-independent lower bounds on the conditional von neumann entropy (2023), arXiv:2106.13692 [quant-ph].
- [59] C. Roch i Carceller *et al.*, In preparation.
- [60] R. Renner, Security of quantum key distribution (2006), arXiv:quant-ph/0512258 [quant-ph].
- [61] J. Bouzitat, *Integration numerique approchee par la methode de Gauss generalisee et extension de cette methode* (Techniques de Calcul Numérique, 1952).
- [62] W. Gautschi and S. Li, Gauss—radau and gauss—lobatto quadratures with double end points, *Journal of Computational and Applied Mathematics* **34**, 343 (1991).

- [63] R. Arnon-Friedman, F. Dupuis, O. Fawzi, R. Renner, and T. Vidick, Practical device-independent quantum cryptography via entropy accumulation, *Nature Communications* **9**, 459 (2018).

## Appendix A: Min-entropy semidefinite program: Primal and Dual

In this section we formally introduce the semidefinite program we use to bound the certifiable randomness using the min-entropy.

### 1. Primal SDP

We start presenting the primal form of the problem. Our goal is to maximise the guessing probability of the eavesdropper which we can write as

$$p_g = \sum_{\lambda} q(\lambda) \max_b \{ \text{Tr} [\rho_2 \pi_b^\lambda] \} . \quad (\text{A1})$$

The maximisation is done through all possible measurement strategies  $\lambda$ , distributions  $q(\lambda)$  and POVM elements  $\pi_b^\lambda$ . These are constrained to be valid distributions and POVMs, which implies

$$q(\lambda) \geq 0 \quad \sum_{\lambda} q(\lambda) = 1 \quad q(\lambda) \in \mathbb{R} \quad (\text{A2})$$

$$\pi_b^\lambda \geq 0 \quad \sum_b \pi_b^\lambda = \mathbb{1} \quad \pi_b^\lambda = (\pi_b^\lambda)^\dagger . \quad (\text{A3})$$

There is the additional constraint that the observed probabilities must be reproduced on the real experiment. This is reflected in

$$p(b|x) = \sum_{\lambda} q(\lambda) \text{Tr} [\rho_x \pi_b^\lambda] . \quad (\text{A4})$$

Since states  $\rho_x$  are not fully specified, but instead only their overlaps are bounded, we will insert the states in (C14), so  $\rho_x = |\tilde{\psi}_x\rangle\langle\tilde{\psi}_x|$ .

This optimisation problem can be rendered as a linear semi-definite program following a couple of steps. First, we will consider only the most relevant strategies, which in our case are those which yield the maximal value  $\max_b \{ \text{Tr} [\rho_x \pi_b^\lambda] \}$ . This can be done by simply labeling  $\lambda = b$  the maximal strategy for outcome  $b$ , i.e.  $\max_b \{ p(b|x=2, \lambda) \} = p(\lambda|x=2, \lambda)$ . This leaves us with only  $n_B$  relevant strategies, being  $n_B$  the number of different outcomes from the measurement. Secondly, we will absorb the distribution  $q(\lambda)$  in the POVM element  $\pi_b^\lambda$  and define a new quantity  $M_b^\lambda = q(\lambda) \pi_b^\lambda$ . The definition of this new operator changes the above constraints to the following:

$$M_b^\lambda \geq 0 \quad , \quad M_b^\lambda = (M_b^\lambda)^\dagger \quad \forall b, \lambda \quad , \quad \sum_b M_b^\lambda = \frac{1}{D} \text{Tr} \left[ \sum_b M_b^\lambda \right] \quad \forall \lambda \quad , \quad (\text{A5})$$

where  $D$  is the dimensionality of the eavesdropper. The useful space accessible by the eavesdropper is that spanned by the states involved in the experiment. Since we are considering a three-state discrimination setting, the dimension can be at maximum the number of states, i.e.  $D = 3$ . The reproducibility constraint is also changed to simply

$$p(b|x) = \sum_{\lambda} \text{Tr} [\rho_x M_b^\lambda] . \quad (\text{A6})$$

Finally, we can re-write the guessing probability in the following way

$$p_g = \sum_{\lambda} \text{Tr} [\rho_2 M_\lambda^\lambda] . \quad (\text{A7})$$

An upper bound  $p_g^* \geq p_g$  can be found by maximising it through all possible  $2 \times 2$  matrices  $M_b^\lambda$  that fulfil the constraints above.

## Appendix B: Shannon entropy see-saw SDP

In this section we present method we used to bound the Shannon entropy and the *see-saw* semidefinite program to numerically compute it.

Consider the prepare-and-measure scenario where Alice draws a classical value  $x$  with probability  $p_x$  which she feeds into a device that prepares a quantum state  $\Psi_x$ . While she sends one part of  $\Psi_x$  (namely  $\rho_x$ ) to Bob, the rest (namely  $\sigma_x$ ) is leaked to the adversary (Eve). Let us label Bob and Eve's Hilbert spaces with  $\mathcal{H}_B$  and  $\mathcal{H}_E$  respectively, such that the global state is  $\Psi_x \in \mathcal{H}_B \otimes \mathcal{H}_E$ ,  $\rho_x := \text{Tr}_E[\Psi_x]$  and  $\sigma_x := \text{Tr}_B[\Psi_x]$ . Then, Bob performs a measurement on  $\rho_x$  in his laboratory, while Eve's goal is to guess Bob's measurement outcome by measuring her part of the state  $\sigma_x$  on her separated laboratory, and also be able to share randomness (through the hidden variable  $\lambda$ ) with Bob's measurement device. Let us call  $\{\Pi_b\}$  the POVM that represents the targeted measurement in Bob's device.

Our first goal is to find an expression to lower-bound the Von Neumann entropy in Bob's measurement outcome relative to Eve. After Bob measures, the whole quantum state shared between Bob and Eve is updated to the classical-quantum state

$$\tilde{\Psi}_x = \sum_b |b\rangle \langle b| \otimes \tilde{\sigma}_x(b). \quad (\text{B1})$$

This means that Bob is left with the classical value  $b$  of his measurement outcome, while Eve's state becomes  $\tilde{\sigma}_x(b) = \text{Tr}_B[(\Pi_b \otimes \mathbf{1})\Psi_x]$ . We can express the Von Neumann entropy of Bob's outcome conditioned on Eve's knowledge for a particular state preparation  $x^*$  in terms of the relative entropy

$$H(B|E, X = x^*) = -D\left(\tilde{\Psi}_{x^*} \parallel \mathbf{1} \otimes \tilde{\sigma}_{x^*}\right), \quad (\text{B2})$$

for  $\tilde{\sigma}_x = \sum_b \tilde{\sigma}_x(b)$ . As shown in Ref. [58], applying the Gauss-Radau quadrature to an integral representation of the logarithm yields a variational upper bound for the quantum relative entropy,

$$D(\rho \parallel \sigma) \leq \sum_{i=1}^{m-1} \frac{w_i}{t_i \log 2} \inf_{Z_i} \left( 1 + \text{Tr} \left[ \rho \left( Z_i + Z_i^\dagger + (1 - t_i) Z_i^\dagger Z_i \right) \right] + t_i \text{Tr} \left[ \sigma Z_i Z_i^\dagger \right] \right), \quad (\text{B3})$$

for  $Z_i$  being arbitrary complex matrices and  $\{w_i, t_i\}$  the weights and nodes from the Gauss-Radau quadrature [61, 62], respectively. In our case, this turns into the following variational lower bound on the Von Neumann entropy for a particular preparation  $x^*$ :

$$H(B|E, X = x^*) \geq c_m + \sum_{i,b} \frac{w_i}{t_i \log 2} \inf_{\{Z_i^b, F_i^b, K_i^b\}} \text{Tr} \left[ \Psi_{x^*} \left( \Pi_b \otimes \left( Z_i^b + Z_i^{b\dagger} + (1 - t_i) F_i^b \right) \right) + t_i \Psi_{x^*} \left( \mathbf{1}_B \otimes K_i^b \right) \right] \quad (\text{B4})$$

where the sum over  $i$  runs from  $i = 1$  to  $i = m - 1$ , and we defined  $c_m = \sum_{i=1}^{m-1} \frac{w_i}{t_i \log 2}$  together with the matrices

$$Z_i^b := \text{Tr}_B \left[ (|b\rangle \langle b| \otimes \mathbf{1}) Z_i \right] \quad (\text{B5})$$

$$F_i^b := \text{Tr}_B \left[ (|b\rangle \langle b| \otimes \mathbf{1}) Z_i^\dagger Z_i \right] \quad (\text{B6})$$

$$K_i^b := \text{Tr}_B \left[ (|b\rangle \langle b| \otimes \mathbf{1}) Z_i Z_i^\dagger \right]. \quad (\text{B7})$$

In our scenario we consider that the eavesdropper has only access to side classical information. Let us label with  $\lambda$  the collection of physical parameters known by Eve which determine the behaviour of Bob's device. This infers that the measurement performed in Bob's device consists of a convex mixture of measurements, determined by the hidden variable  $\lambda$  distributed according to  $q(\lambda)$  and publicly announced to Eve, i.e.  $\Pi_b = \sum_\lambda q(\lambda) \pi_b^\lambda \otimes |\lambda\rangle \langle \lambda|$ . In this case, after Bob performs his measurement, Eve's part of the state updates to  $\tilde{\sigma}_x(b) = \sum_\lambda q(\lambda) \text{Tr}[\rho_x \pi_b^\lambda] |\lambda\rangle \langle \lambda|$ . Let us use these to directly translate the bound on the Von Neumann entropy from (B4) into

$$H(B|E, X = x^*) \geq c_m + \sum_{i=1}^{m-1} \frac{w_i}{t_i \log 2} \inf_{z_i^{\lambda b}, \eta_i^{\lambda b}} \sum_{b,\lambda} q(\lambda) \text{Tr} \left[ \pi_b^\lambda \rho_{x^*} \right] \left( z_i^{\lambda b} + z_i^{\lambda b*} + (1 - t_i) \eta_i^{\lambda b} \right) + q(\lambda) t_i \eta_i^{\lambda b}, \quad (\text{B8})$$

where we introduced the following scalar variables

$$z_i^{\lambda b} := \text{Tr} \left[ (|b\rangle \langle b| \otimes |\lambda\rangle \langle \lambda|) Z_i \right] \quad (\text{B9})$$

$$\eta_i^{\lambda b} := \text{Tr} \left[ (|b\rangle \langle b| \otimes |\lambda\rangle \langle \lambda|) Z_i^\dagger Z_i \right] = \text{Tr} \left[ (|b\rangle \langle b| \otimes |\lambda\rangle \langle \lambda|) Z_i Z_i^\dagger \right], \quad (\text{B10})$$

defined from projecting the arbitrary matrices  $Z_i$  onto  $|b\rangle\langle b|$  and  $|\lambda\rangle\langle\lambda|$  in Bob and Eve's laboratories, respectively. Observe that these definitions imply that all scalars  $z_i^{\lambda b}$  and  $\eta_i^{\lambda b}$  are constrained to fulfil

$$\begin{pmatrix} 1 & z_i^{\lambda b} \\ (z_i^{\lambda b})^* & \eta_i^{\lambda b} \end{pmatrix} \geq 0. \quad (\text{B11})$$

One can see that by constructing the completely positive channel  $\Lambda_{b,\lambda}[M] := \text{Tr}[(|b\rangle\langle b| \otimes |\lambda\rangle\langle\lambda|)M]$ , which consists of a projection onto classical outputs  $b$  and  $\lambda$ . Applying this channel through each element of the strictly positive-semidefinite matrix  $P_i := |\tau_i\rangle\langle\tau_i|$  built from the inner product of vectors  $|\tau_i\rangle := (\mathbf{1}, Z_i)$  yields the matrix in (B11), which by definition must be positive-semidefinite.

In order to find a lower bound on the Shannon entropy, we need to minimise the right-hand side of (B8). To do so, we will employ a *see-saw* method which consists in minimising (B8) alternating between optimisation variables, allowing us to define two different SDPs in each run. The method works as follows:

**Step 1:** Initialise random  $M_b^\lambda = q(\lambda)\bar{\pi}_b^\lambda$

**Step 2:** Compute the new value of  $S^*$  running the following SDP, optimising over  $\{z_i^{\lambda b}, \eta_i^{\lambda b}\}$

$$S^* = \underset{\{z_i^{\lambda b}, \eta_i^{\lambda b}\}}{\text{minimize}} \quad c_m + \sum_{i=1}^{m-1} \frac{w_i}{t_i \log 2} \sum_{b,\lambda} \text{Tr}[M_b^\lambda \rho_{x^*}] (2z_i^{\lambda b} + (1-t_i)\eta_i^{\lambda b}) + \frac{1}{D} \text{Tr} \left[ \sum_{b'} M_{b'}^\lambda \right] t_i \eta_i^{\lambda b} \quad (\text{B12})$$

$$\text{subject to} \quad \Gamma_{b,\lambda,i} = \begin{pmatrix} 1 & z_i^{\lambda b} \\ z_i^{\lambda b} & \eta_i^{\lambda b} \end{pmatrix} \geq 0$$

**Step 3:** Fix  $\{z_i^{\lambda b}, \eta_i^{\lambda b}\}$  from the solution of the SDP.

**Step 4:** Compute the new value of  $S^*$  running the following SDP, optimising over  $\{M_b^\lambda\}$

$$S^* = \underset{\{M_b^\lambda\}}{\text{minimize}} \quad c_m + \sum_{i=1}^{m-1} \frac{w_i}{t_i \log 2} \sum_{b,\lambda} \text{Tr}[M_b^\lambda \rho_{x^*}] (2z_i^{\lambda b} + (1-t_i)\eta_i^{\lambda b}) + \frac{1}{D} \text{Tr} \left[ \sum_{b'} M_{b'}^\lambda \right] t_i \eta_i^{\lambda b} \quad (\text{B13})$$

$$\text{subject to} \quad M_b^\lambda \geq 0, \quad \sum_b M_b^\lambda = \frac{1}{D} \text{Tr} \left[ \sum_b M_b^\lambda \right] \mathbf{1}, \quad \sum_\lambda \text{Tr}[\rho_x M_b^\lambda] = p(b|x)$$

**Step 5:** Fix  $\{M_b^\lambda\}$  from the solution of the SDP and go to **Step 2**.

The whole see-saw optimisation runs over a limited number of rounds  $n$  and we store the average difference between solutions in consecutive rounds, i.e.  $\Delta_k := \sum_{r=n(1+k)}^{nk} |S_r^* - S_{r+1}^*|/n$ , for  $k = 0, 1, 2, \dots$ . The process is repeated as long as this difference is lower than a critical point (chosen to be  $\Delta_k \geq 10^{-4}$ ) or unless a critical  $k$  is reached, at which point the algorithm is re-started with an alternative random point.

### Appendix C: Unconstrained dimensionality and semi-device independence

In this section, we show how bounding the overlaps between the prepared states can limit this the use of any additional dimension by the eavesdropper.

Consider the state discrimination scenario with three preparations. Two of the prepared states  $|\tilde{\psi}_0\rangle$  and  $|\tilde{\psi}_1\rangle$  have support only on a two-dimensional Hilbert space, but the third state  $|\tilde{\psi}_2\rangle$  may have support also on a third dimension.

Then,

$$|\tilde{\psi}_0\rangle = \cos \frac{\phi}{2} |0\rangle + \sin \frac{\phi}{2} |1\rangle + 0 |2\rangle \quad (\text{C1})$$

$$|\tilde{\psi}_1\rangle = \cos \frac{\phi}{2} |0\rangle - \sin \frac{\phi}{2} |1\rangle + 0 |2\rangle \quad (\text{C2})$$

$$|\tilde{\psi}_2\rangle = \sqrt{a} \left( \cos \frac{\theta}{2} |0\rangle + e^{i\varphi} \sin \frac{\theta}{2} |1\rangle \right) + \sqrt{1-a} |2\rangle \quad (\text{C3})$$

Suppose now that we only trust a bound on the overlap of the prepared states. Let us define  $|\langle \tilde{\psi}_0 | \tilde{\psi}_1 \rangle| \geq |d_{01}|$ ,  $|\langle \tilde{\psi}_0 | \tilde{\psi}_2 \rangle| \geq |d_{02}|$  and  $|\langle \tilde{\psi}_1 | \tilde{\psi}_2 \rangle| \geq |d_{12}|$ . This means that

$$\left| \langle \tilde{\psi}_0 | \tilde{\psi}_2 \rangle \right|^2 = a \left( \cos \frac{\phi}{2} \cos \frac{\theta}{2} + e^{i\varphi} \sin \frac{\phi}{2} \sin \frac{\theta}{2} \right) \left( \cos \frac{\phi}{2} \cos \frac{\theta}{2} + e^{-i\varphi} \sin \frac{\phi}{2} \sin \frac{\theta}{2} \right) \quad (\text{C4})$$

$$= a \left( \cos^2 \frac{\phi}{2} \cos^2 \frac{\theta}{2} + \sin^2 \frac{\phi}{2} \sin^2 \frac{\theta}{2} + (e^{i\varphi} + e^{-i\varphi}) \cos \frac{\phi}{2} \cos \frac{\theta}{2} \sin \frac{\phi}{2} \sin \frac{\theta}{2} \right) \quad (\text{C5})$$

$$= \frac{a}{2} (1 + \cos \phi \cos \theta + \sin \varphi \sin \phi \sin \theta) \quad (\text{C6})$$

$$\left| \langle \tilde{\psi}_1 | \tilde{\psi}_2 \rangle \right|^2 = \dots = \frac{a}{2} (1 + \cos \phi \cos \theta - \sin \varphi \sin \phi \sin \theta) \quad (\text{C7})$$

$$\left| \langle \tilde{\psi}_0 | \tilde{\psi}_2 \rangle \right|^2 + \left| \langle \tilde{\psi}_1 | \tilde{\psi}_2 \rangle \right|^2 = a (1 + \cos \phi \cos \theta) \geq |d_{02}|^2 + |d_{12}|^2 \quad (\text{C8})$$

$$a \geq \frac{d_{02}^2 + d_{12}^2}{1 + d_{01} \cos \theta} \quad (\text{C9})$$

If  $a = 1$ , the three states will have support on the same bi-dimensional Hilbert space. Whilst the measurement device is treated as a black box, the preparation device is partially characterized through the bounds we place on the overlaps of the prepared states. Then, the eavesdropper has the freedom in choosing the states  $|\psi_x\rangle$  in terms of the angles  $\phi$ ,  $\theta$  and  $\varphi$  that satisfy those bounds. Her probability of guessing the measurement outcome when state  $|\tilde{\psi}_2\rangle$  is prepared is

$$\begin{aligned} p_g &= \sum_{\lambda} q(\lambda) \max_b \left\{ \langle \tilde{\psi}_2 | \pi_b^\lambda | \tilde{\psi}_2 \rangle \right\} \\ &= \sum_{\lambda} q(\lambda) \max_b \left\{ a \langle \psi_2 | \pi_b^\lambda | \psi_2 \rangle + (1-a) \langle 2 | \pi_b^\lambda | 2 \rangle + \sqrt{a(1-a)} (\langle \psi_2 | \pi_b^\lambda | 2 \rangle + \langle 2 | \pi_b^\lambda | \psi_2 \rangle) \right\}. \end{aligned} \quad (\text{C10})$$

The support of the POVM onto the qubit space spanned by the test states  $|\tilde{\psi}_0\rangle$  and  $|\tilde{\psi}_1\rangle$  is constrained by the reproducibility of the observed statistics  $p(b|x)$ . However, the support onto the sub-space spanned by  $|2\rangle$  does not have any constraints applied. This implies that  $p_g$  is maximum whenever the measurement described by the POVM  $\{\pi_b^\lambda\}$  has minimal support on the constrained subspace. Thus, the upper bound on  $p_g$  is given whenever  $a$  is minimal, which we know is lower bounded indirectly by (C4) whenever the overlaps of the prepared states are also bounded.

On the SDP this is reflected by considering the discrimination of the qutrit states  $|\tilde{\psi}_x\rangle$ . Assume that Eve is even allowed to change the angles  $\phi$  and  $\theta$ , so that the bounds on the overlaps are still satisfied. Eve can pick them to be the ones she wants in order to make the support onto the third dimension as large as she can. Let's see what is the best she can do. We first relate both angles in a single expression by first writing  $a = (d_{02}^2 - d_{12}^2) / (\sqrt{1 - d_{01}^2} \sin \theta \cos \varphi)$  and equating with the right-hand side in (C4). One gets

$$\cos \varphi = \frac{d_{02}^2 - d_{12}^2}{d_{02}^2 + d_{12}^2} \frac{1 + d_{01} \cos \theta}{\sqrt{1 - d_{01}^2} \sin \theta}. \quad (\text{C11})$$

If one plots  $\cos \theta$  vs.  $\cos \varphi$ , one will see that: if  $d_{02} > d_{12}$ ,  $\cos \theta$  is maximal if  $\cos \varphi = 1$ ; if  $d_{02} < d_{12}$ ,  $\cos \theta$  is maximal if  $\cos \varphi = -1$ ; and if  $d_{02} = d_{12}$ ,  $\cos \theta$  is maximal if  $\cos \varphi = 0$ . The maximal value of  $\cos \theta$  is the same in the three cases, being

$$(\cos \theta)_{\max} = \frac{2d_{02}d_{12} - d_{01}(d_{02}^2 + d_{12}^2)}{d_{02}^2 - 2d_{01}d_{02}d_{12} + d_{12}^2}, \quad (\text{C12})$$

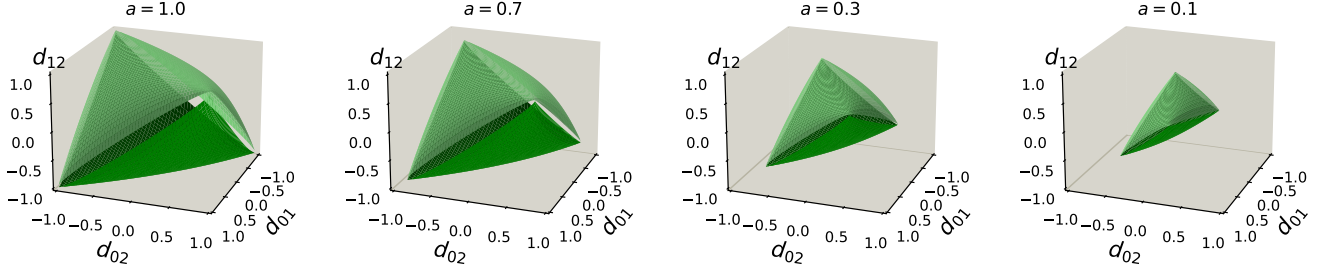


FIG. 5. Tetrahedron formed by the available overlap configurations in the preparation of three non-orthogonal quantum states. The parameter  $a$  indicates the minimal support of the prepared states onto a two-dimensional subspace if only their overlaps are bounded.

which means

$$a \geq \frac{d_{02}^2 + d_{12}^2 - 2d_{01}d_{02}d_{12}}{1 - d_{01}^2}. \quad (\text{C13})$$

Equation (C13) defines the surface of a tetrahedron with curved faces. The amplitude  $a$  decreases towards the center of the tetrahedron non-symmetrically, as we show in Fig. 5.

On the SDP, the prepared states shall only be expressed in terms of the bounds of the overlaps  $d_{xy}$ , which can be done by replacing the angles  $\phi$ ,  $\theta$  and  $\varphi$  with  $d_{01}$ ,  $d_{02}$  and  $d_{12}$  accordingly. This yields

$$\begin{aligned} |\tilde{\psi}_0\rangle &= \sqrt{\frac{1+d_{01}}{2}} |0\rangle + \sqrt{\frac{1-d_{01}}{2}} |1\rangle + 0 |2\rangle \\ |\tilde{\psi}_1\rangle &= \sqrt{\frac{1+d_{01}}{2}} |0\rangle - \sqrt{\frac{1-d_{01}}{2}} |1\rangle + 0 |2\rangle \\ |\tilde{\psi}_2\rangle &= \frac{1}{\sqrt{2}} \frac{d_{02} + d_{12}}{\sqrt{1+d_{01}}} |0\rangle + \frac{1}{\sqrt{2}} \frac{d_{02} - d_{12}}{\sqrt{1-d_{01}}} |1\rangle + \sqrt{1 - \frac{|d_{02} + d_{12}|^2}{2(1+d_{01})} - \frac{|d_{02} - d_{12}|^2}{2(1-d_{01})}} |2\rangle. \end{aligned} \quad (\text{C14})$$

A particular choice of bounds on the overlaps and their phases limits the accessibility to a the third dimension by Eve. Concretely, one can tune the states to be symmetric in the sense that  $d_{02} = d_{12}^* = \tilde{d}e^{i\gamma}$ . Thus, fulfilling the relation  $\tilde{d}^2 = (1 - d_{01}^2)/(2(1 - d_{01} \cos 2\gamma))$  makes the third component of  $|\tilde{\psi}_2\rangle$  null. This means that we can be sure that any potential eavesdropper will gain no information of the outcome by reaching into an additional third dimension.

#### Appendix D: Implementations: specific details

In this section of the appendix we detail the specific parameters to be adjusted to obtain the desired statistics in the measurement outcomes on the proposed implementation.

The proposed implementation for the USD setup consists in preparing the equi-probable two-mode coherent states  $|\psi_0\rangle = |\alpha\rangle \otimes |0\rangle$  and  $|\psi_1\rangle = |0\rangle \otimes |\alpha\rangle$ . These can be unambiguously discriminated by means of using only photo detectors in each mode. If only the photo detector in the first mode clicks, that would mean that state  $|\alpha 0\rangle$  had been prepared, and thus, we associate the outcome  $b = 0$ . Otherwise, if only the second photo-detector clicks, means that  $|0\alpha\rangle$  was prepared and we associate  $b = 1$  as a measurement outcome. Note that if these two states are prepared, there is a possibility that none of the detectors click. If that happens, the measurement is uncertain of which state was prepared and we associate this events with the inconclusive measurement outcome  $b = 2$ . Assume now that we include the preparation of a third two-mode coherent state  $|\psi_2\rangle = |\beta_0\beta_1\rangle$  into play. Whenever this state is prepared, either only one detector can click, the other, none or even both at the same time. Let us go through all possible

measurement events and their probabilities to happen whenever a generic state  $|\psi_x\rangle$  is prepared.

$$\begin{aligned}
1 &= \langle \psi_x | (\mathbf{1} \otimes \mathbf{1}) | \psi_x \rangle = \langle \psi_x | \left( \sum_{n=0}^{\infty} |n\rangle \langle n| \right) \otimes \left( \sum_{m=0}^{\infty} |m\rangle \langle m| \right) | \psi_x \rangle \\
&= \langle \psi_x | \left( |0\rangle \langle 0| + \sum_{n=1}^{\infty} |n\rangle \langle n| \right) \otimes \left( |0\rangle \langle 0| + \sum_{m=1}^{\infty} |m\rangle \langle m| \right) | \psi_x \rangle \tag{D1} \\
&= \langle \psi_x | \left( \underbrace{|0\rangle \langle 0| \otimes |0\rangle \langle 0|}_{\text{Detector doesn't click}} + \underbrace{|0\rangle \langle 0| \otimes \sum_{m=1}^{\infty} |m\rangle \langle m|}_{\text{Click on late bin}} + \underbrace{\sum_{n=1}^{\infty} |n\rangle \langle n| \otimes |0\rangle \langle 0|}_{\text{Click on early bin}} + \underbrace{\sum_{n=1}^{\infty} |n\rangle \langle n| \otimes \sum_{m=1}^{\infty} |m\rangle \langle m|}_{\text{Click on both early and late bins}} \right) | \psi_x \rangle \\
&= |\langle 00 | \psi_x \rangle|^2 + \sum_{m=1}^{\infty} |\langle 0m | \psi_x \rangle|^2 + \sum_{n=1}^{\infty} |\langle n0 | \psi_x \rangle|^2 + \sum_{n=1}^{\infty} \sum_{m=1}^{\infty} |\langle nm | \psi_x \rangle|^2 .
\end{aligned}$$

The event consisting in a simultaneous click at both time-bins does not come into play when unambiguously discriminating the two-mode coherent states  $|\alpha 0\rangle$  and  $|0 \alpha\rangle$ . In fact, that event would correspond in a unambiguous identification of the third state  $|\beta_0 \beta_1\rangle$ . Since our aim is to only consider measurement strategies able to unambiguously discriminate solely states  $|\alpha 0\rangle$  and  $|0 \alpha\rangle$ , whenever that event occurs we will consider that  $b = 0$  with probability  $g_0$ ,  $b = 1$  with the same probability  $g_1$  and the rest of the times  $b = 2$  with probability  $g_2$ . No data will be discarded so that the certified randomness is not affected. The considered events and their corresponding probabilities depending on which state was prepared after the post-processing are summarized in table I.

Prepared state \ Meas. Event	$b = 0$	$b = 1$	$b = 2$
$ \psi_0\rangle =  \alpha\rangle \otimes  0\rangle$	$1 - e^{- \alpha ^2}$	0	$e^{- \alpha ^2}$
$ \psi_1\rangle =  0\rangle \otimes  \alpha\rangle$	0	$1 - e^{- \alpha ^2}$	$e^{- \alpha ^2}$
$ \psi_2\rangle =  \beta_0\rangle \otimes  \beta_1\rangle$	$\begin{aligned} & (1 - e^{- \beta_0 ^2}) e^{- \beta_1 ^2} \\ & + g_0 (1 - e^{- \beta_0 ^2}) (1 - e^{- \beta_1 ^2}) \end{aligned}$	$\begin{aligned} & e^{- \beta_0 ^2} (1 - e^{- \beta_1 ^2}) \\ & + g_1 (1 - e^{- \beta_0 ^2}) (1 - e^{- \beta_1 ^2}) \end{aligned}$	$\begin{aligned} & e^{- \beta_0 ^2} e^{- \beta_1 ^2} \\ & + g_2 (1 - e^{- \beta_0 ^2}) (1 - e^{- \beta_1 ^2}) \end{aligned}$

TABLE I. Summary of the considered measurement events and their corresponding re-normalized probabilities for the USD setup.

For simplicity and without loss of generality, we will consider non-imaginary coherent amplitudes only. The overlaps of the prepared states are characterized by the amplitudes of the coherent states as follows

$$d_{01} = e^{-\alpha^2} \quad d_{02} = e^{-\frac{(\alpha-\beta_0)^2}{2}} e^{-\frac{\beta_1^2}{2}} \quad d_{12} = e^{-\frac{\beta_0^2}{2}} e^{-\frac{(\alpha-\beta_1)^2}{2}} . \tag{D2}$$

Over a set of runs, we observed that the best and simplest choice is to pick  $g_0 = g_1 = 1/2$  and so  $g_2 = 0$ .

### Appendix E: Finite size effects and entropy accumulation

In this section we explain how we treat finite size effects from the data extracted in the experiment. Also, we explain how we can abandon the general assumption of independent and identically distributed rounds (i.i.d) though the entropy accumulation theorem (EAT) as is explained in [63].

#### 1. Finite-size effects under the i.i.d. assumption: Asymptotic Equipartition Property

In the real life implementation of the protocol, the observed statistics are built from finite sets of collected data. Thus, the entropy is computed based on a finite number of samples. In order to incorporate such finite-size effects



into our analysis, we make use of the asymptotic equipartition property (AEP) generalised to the quantum theory [47]. This allows us to quantify the amount of certifiable randomness over a fixed number of experiment rounds assuming these are independent and identically distributed (i.i.d.). From the experiment we collect pairs of data-points for each question (or state preparation  $x$ ) and answer (measurement outcome  $b$ ). We label by  $n_{b,x}$  the number of pairs with question  $x$  and answer  $b$ . Then, from the set of questions we label  $n_x$  the number of questions  $x$ , and from the set of answers we label  $n_b$  the number of answers  $b$ . The total number of extracted data-points is  $N = \sum_b n_b = \sum_x n_x = \sum_{b,x} n_{b,x}$ . From these, we can obtain the observed frequencies as  $\text{freq.}(b|x) = n_{b,x}/\sum_b n_{b,x}$ . Then, we can compute the single round Shannon entropy using the see-saw optimisation method introduced in App. B. The quantum AEP then states that the smooth-min-entropy ( $H_{\min}^\varepsilon(B^N|E^N)$ ) per-round can be bounded using the following expression

$$\frac{1}{N} H_{\min}^\varepsilon(B^N|E^N) \geq H(B|E) - \frac{\delta(\varepsilon, \eta^{\text{AEP}})}{\sqrt{N}}, \quad (\text{E1})$$

where the Von Neumann entropy  $H(B|E)$  in our case is reduced to the Shannon entropy per-round, and

$$\delta(\varepsilon, \eta^{\text{AEP}}) := 4 \log \eta^{\text{AEP}} \sqrt{\log \frac{2}{\varepsilon^2}} \quad \text{with} \quad \eta^{\text{AEP}} \leq \sqrt{2^{-H_{\min}(B|E)}} + \sqrt{2^{H_{\max}(B|E)}} + 1. \quad (\text{E2})$$

To compute the max-entropy  $H_{\max}(B|E)$  we use the results from Ref. [46]. Specifically, for any separable bi-partite state shared between Bob and Eve  $\rho_{BE} = \rho_B \otimes \rho_E$ , the max-entropy can be obtained as

$$H_{\max}(B|E) = 2 \log \text{Tr}[\sqrt{\rho_B}]. \quad (\text{E3})$$

Indeed, our assumptions on the state preparations (i.e. bounded overlaps and pure states) fit within this case. We thus have all essential ingredients to compute a bound on the smooth-min-entropy per-round using (E1) in the i.i.d. case.

## 2. Entropy accumulation theorem: dropping the i.i.d. assumption

The i.i.d. assumption is not very attractive in (semi-)device independent protocols. Indeed, this assumes that the eavesdropper cannot learn from past rounds to have a better guess in future rounds (sort of as if the eavesdropper loses its memory in each round). To get rid of this strong assumption, we refer to the entropy accumulation theorem (EAT) generalised to prepare-and-measure scenarios [48] and its application in [49]. Here we adapt it to our semi-device independent prepare-and-measure scenario. The EAT places a bound on the *smooth*-min-entropy, that is the maximum min-entropy of a distribution  $\varepsilon$ -close to the target distribution, per round in a prepare-and-measure experiment with  $N$  rounds. The EAT implies that the operationally total relevant uncertainty about the total set of outcomes over  $N$  rounds  $B_1^N$  corresponds to the sum of the entropies of the individual rounds to first order in  $N$  under the i.i.d. assumption, plus a contribution from not assuming the i.i.d. case. This contribution is provided given that one quantifies the uncertainty of each individual round with the Von Neumann entropy of a suitable chosen state. Formally, the generalised EAT reads

$$\frac{1}{N} H_{\min}^\varepsilon(B^N|E^N) \geq \min_{c_N \in \Omega} f(\text{freq.}(c_N)) - \frac{\alpha - 1}{2 - \alpha} \frac{\ln(2)}{2} V^2 - \frac{1}{N} \frac{g(\varepsilon) + \alpha \log(1/\text{Pr}[\Omega])}{\alpha - 1} - \left(\frac{\alpha - 1}{2 - \alpha}\right)^2 K'(\alpha). \quad (\text{E4})$$

Several new elements appear in (E4), let us properly introduce them one by one. First,  $f$  is a so-called *trade-off function* and it is defined as an analytical function on the observed frequencies ( $\text{freq.}(c_N)$ ) computed on the events whenever randomness is certified ( $c_N$ ) such that it lower-bounds the minimum entropy over all possible post-measurement states. Namely,

$$f(q) \leq \min_{\nu \in \Sigma_i(q)} H(B_i|E_i)_\nu \quad (\text{E5})$$

for  $\Sigma_i(q)$  being the set of states that can be generated after the measurement at the  $i^{\text{th}}$  experiment round given the observed frequencies  $q$ . The lower bound in (E4) is computed on the minimum  $f$  over the total number of observed events  $c_N$  belonging to a particular chosen event  $\Omega$ , e.g. the winning condition in non-local games. In our case  $\Omega$  represents all events where we certify randomness, i.e. whenever  $x = 2, \forall b$ , occurring with probability

$\Pr(\Omega) = p_{x=2} = 1/2$ . Also, from the trade-off function we need to compute the maximum  $\text{Max}(f)$ , minimum  $\text{Min}(f)$  and its variance  $\text{Var}(f)$ . These are then used to compute the following quantities

$$g(\varepsilon) = -\log(1 - \sqrt{1 - \varepsilon^2}) , \quad (\text{E6})$$

$$V = \log(2n_B^2 + 1) + \sqrt{2 + \text{Var}(f)} , \quad (\text{E7})$$

$$K'(\alpha) = \frac{(2 - \alpha)^3}{6(3 - 2\alpha)^3 \ln(2)} 2^{\frac{\alpha-1}{2-\alpha}(2 \log n_B + \text{Max}(f) - \text{Min}(f))} \ln^3 \left( 2^{2 \log n_B + \text{Max}(f) - \text{Min}(f)} + e^2 \right) , \quad (\text{E8})$$

with  $n_B$  corresponding to the number of measurement outcomes. Finally, the bound in (E4) is originally derived using some appropriate properties of the Reny entropies  $H_\alpha$  for  $\alpha \in (1, 2)$ . We thus set  $\alpha = 1 + \mathcal{O}(1/\sqrt{N})$  which is entirely motivated by Ref [48], so that one gets a correction term  $\mathcal{O}(1/\sqrt{N})$  in the bound on the certifiable entropy per-round.

The next step is to find a good candidate for  $f$ . Recall that using the see-saw optimisation in App. B we are already obtaining a lower-bound on the Shannon entropy and thus, we find suitable to use this result as  $f$ , fulfilling (E5). Next, since statistical correlations are fixed by observation, this lower-bound already takes into account the minimisation  $\forall c_N \in \Omega$  in (E4). Translated to our experiment, in summary, we use the output of the see-saw optimisation  $S^*$  as

$$S^* = \min_{c_N \in \Omega} f(\text{freq.}(c_N)) , \quad (\text{E9})$$

which again, by definition, fulfils (E5).

---